

University of Plymouth

PEARL

<https://pearl.plymouth.ac.uk>

Faculty of Health: Medicine, Dentistry and Human Sciences

School of Biomedical Sciences

2016-09-01

Accepted Manuscript

Palmitate-induced changes in energy demand cause reallocation of ATP supply in rat and human skeletal muscle cells

Raid B. Nisr, Charles Affourtit

PII: S0005-2728(16)30385-1
DOI: doi: [10.1016/j.bbabbio.2016.04.286](https://doi.org/10.1016/j.bbabbio.2016.04.286)
Reference: BBABIO 47683

To appear in: *BBA - Bioenergetics*

Received date: 1 February 2016
Revised date: 16 April 2016
Accepted date: 28 April 2016



Please cite this article as: Raid B. Nisr, Charles Affourtit, Palmitate-induced changes in energy demand cause reallocation of ATP supply in rat and human skeletal muscle cells, *BBA - Bioenergetics* (2016), doi: [10.1016/j.bbabbio.2016.04.286](https://doi.org/10.1016/j.bbabbio.2016.04.286)

This is a PDF file of an unedited manuscript that has been accepted for publication. As a service to our customers we are providing this early version of the manuscript. The manuscript will undergo copyediting, typesetting, and review of the resulting proof before it is published in its final form. Please note that during the production process errors may be discovered which could affect the content, and all legal disclaimers that apply to the journal pertain.

Palmitate-induced changes in energy demand cause reallocation of ATP supply in rat and human skeletal muscle cells

Raid B. Nisr¹ and Charles Affourtit^{1,2}

¹School of Biomedical & Healthcare Sciences, Plymouth University, Drake Circus, PL4 8AA, Plymouth, UK

²*Corresponding author*

School of Biomedical and Healthcare Sciences, Plymouth University, Drake Circus, PL4 8AA, Plymouth, United Kingdom

Tel. +44 (0)1752 584649

Fax. +44 (0)1752 584605

Email charles.affourtit@plymouth.ac.uk

Abstract: Mitochondrial dysfunction has been associated with obesity-related muscle insulin resistance, but the causality of this association is controversial. The notion that mitochondrial oxidative capacity may be insufficient to deal appropriately with excessive nutrient loads is for example disputed. *Effective* mitochondrial capacity is indirectly, but largely determined by ATP-consuming processes because skeletal muscle energy metabolism is mostly controlled by ATP demand. Probing the bioenergetics of rat and human myoblasts in real time we show here that the saturated fatty acid palmitate lowers the rate and coupling efficiency of oxidative phosphorylation under conditions it causes insulin resistance. Stearate affects the bioenergetic parameters similarly, whereas oleate and linoleate tend to decrease the rate but not the efficiency of ATP synthesis. Importantly, we reveal that palmitate influences how oxidative ATP supply is used to fuel ATP-consuming processes. Direct measurement of newly made protein demonstrates that palmitate lowers the rate of *de novo* protein synthesis by more than 30%. The anticipated decrease of energy demand linked to protein synthesis is confirmed by attenuated cycloheximide-sensitivity of mitochondrial respiratory activity used to make ATP. This indirect measure of ATP turnover indicates that palmitate lowers ATP supply reserved for protein synthesis by at least 40%. This decrease is also provoked by stearate, oleate and linoleate, albeit to a lesser extent. Moreover, palmitate lowers ATP supply for sodium pump activity by 60-70% and, in human cells, decreases ATP supply for DNA/RNA synthesis by almost three-quarters. These novel fatty acid effects on energy expenditure inform the 'mitochondrial insufficiency' debate.

Keywords: palmitate-induced insulin resistance, skeletal muscle, mitochondrial dysfunction, ATP turnover, obesity, type 2 diabetes

1. INTRODUCTION

Obesity and insulin resistance are related features of the Metabolic Syndrome, a cluster of medical disorders that increase the risk of developing type 2 diabetes and cardiovascular disease [1]. Increased insulin secretion by the pancreatic beta cells may compensate insulin resistance of skeletal muscle and the liver initially, but the obese state often also provokes beta cell dysfunction [2], which largely accounts for the persistently high blood glucose level that characterises type 2 diabetes [3]. The molecular mechanisms that link obesity to insulin resistance are yet to be established conclusively but likely involve excess dietary nutrients, peptide hormones and inflammatory molecules [4]. Non-esterified fatty acids (NEFAs¹) are for example relatively abundant in the circulation of obese subjects [5], and exposure of skeletal muscle and myocytes to free fatty acids – saturated long-chain species such as palmitate and stearate in particular – causes insulin resistance [6].

The mechanism by which free fatty acids dampen the insulin sensitivity of skeletal muscle is not fully understood, but NEFA-induced insulin resistance has been associated firmly with mitochondrial dysfunction [7-9]. However, the causality of this association remains subject of fierce debate [10,11]. It is highly conceivable that the oxidative capacity of muscle cells in obese subjects is insufficient to burn the elevated NEFA supply effectively [7,12] and thus causes accumulation of metabolites that blunt insulin responsiveness. Molecules suggested to interfere with insulin signalling include lipid species such as ceramide and diacylglycerol [13,14], and mitochondrial reactive oxygen species (ROS) [15-17]. Despite experimental evidence in its favour [10], the 'mitochondrial insufficiency' model does not enjoy unanimous support [8,11]. Various rodent models of severe mitochondrial dysfunction for example exhibit improved rather than impaired muscle insulin sensitivity [18-20], and fat oxidation capacity tends to be increased, not decreased, in obese/insulin-resistant and type 2 diabetic subjects [11]. Moreover, type 2 diabetic patients increase their substrate oxidation rate some 40-fold in response to exercise [11]. Based on this sizeable response, it has been reasoned [11] that obese subjects should have enough spare respiratory capacity to fully oxidise any excess lipid.

The capacity of a biological system to burn metabolic fuel depends on the way it controls its energy metabolism. Arguably the most important parameter in cellular bioenergetics is the

¹ *Abbreviations:* AHA, L-azidohomoalanin; 2DG, 2-deoxyglucose; BSA, bovine serum albumin; DMEM, Dulbecco's modified Eagle medium; FCCP, trifluorocarbonylcyanide phenylhydrazone; FBS, fetal bovine serum; HEPES, 4-(2-hydroxyethyl)-1-piperazineethanesulfonic acid; KRPH, Krebs Ringer Phosphate HEPES buffer; NEFA, non-esterified fatty acid; PBS, phosphate-buffered saline; RFU, relative fluorescence units; ROS, reactive oxygen species

ATP/ADP ratio, as it is this phosphorylation potential that allow cells to perform work [21]. In muscle cells, the ATP/ADP ratio is mostly controlled by ATP demand, a paradigm [21] that is acknowledged by both proponents and opponents of the 'mitochondrial insufficiency' model [10,11]. Such distribution of control implies that the rate of ATP supply, and hence oxidative phosphorylation, is fully governed by ATP turnover. In other words, any spare respiratory capacity of a muscle cell will be inconsequential if there is no demand for ATP. Indeed, many paradoxical observations in the insulin resistance literature are readily reconciled by considering the variable energetic needs of the different experimental systems studied [8]. As cellular energy demand clearly influences how lipids affect insulin sensitivity [8], we deemed it important to establish whether or not NEFA exposure had any effect on the ATP requirements of skeletal muscle cells.

In this paper we report that palmitate-induced insulin resistance of rat and human skeletal muscle cells associates with a decreased rate and efficiency of oxidative phosphorylation, and, importantly, with an inhibition of major ATP-consuming processes. These data suggest that the lowered ATP supply is partly owing to decreased ATP turnover.

2. MATERIAL AND METHODS

2.1 Cell culture

Rat L6 myoblasts were obtained from the European Collection of Cell Culture and were maintained at 37 °C under a humidified carbogen atmosphere in Dulbecco's Modified Eagle Medium (DMEM – LifeTechnology 42430-025) containing 25 mM glucose and 20 mM Hepes (4-(2-hydroxyethyl)-1-piperazineethanesulfonic acid) and supplemented with 10% (v/v) FBS (fetal bovine serum), 100 U/mL penicillin, and 100 µg/mL streptomycin. Cells between passages 18 and 25 were used for experimentation. As described in detail before [22], human myoblasts were isolated and cultured at the University of Exeter Medical School, St Luke's Campus (Human Tissue Authority licence 12104), and passaged at least twice before off-site analysis. Needle biopsies to remove skeletal muscle (*vastus lateralis*) tissue were taken with informed donor consent and with approval from the Ethics Committee of the Department of Sport and Health Sciences, College of Life and Environmental Sciences, University of Exeter, UK. Human muscle cells were maintained at 37 °C under a humidified carbogen atmosphere in DMEM (Life Technology 22320-22) containing 5 mM glucose and 20 mM Hepes and supplemented with 20% (v/v) FBS, 0.5% (v/v) chick embryo extract, 2 nM insulin, 100 U/mL penicillin, and 100 µg/mL streptomycin. The initial cell population was

allowed to double 4x before experimentation, and all assays were performed before the population had doubled 10x.

2.2 Fatty acids

Prior to NEFA exposure, cells were nutrient-restricted for 10 or 24 h (glucose uptake and cellular bioenergetics assays, respectively) in DMEM (Life Technology 22320-22) containing just 5 mM glucose and supplemented with only 2% (v/v) FBS to sensitise the cells to insulin [22,23]. NEFAs were administered in conjugation to fatty-acid-free bovine serum albumin (BSA – Sigma A7030) as described previously [22], and cells were exposed to BSA-conjugated NEFAs or to BSA alone for 16 h in DMEM (Life Technology 22320-22) without added FBS. NEFA:BSA conjugates were applied at molar ratios to yield estimated free NEFA levels of approximately 20 nM [24].

2.3 Insulin resistance

Insulin sensitivity was measured as the response of 2-deoxyglucose (2DG) uptake to 100 nM insulin as described previously [22]. The estimated free palmitate concentration of 20 nM rendered both L6 and human myoblasts insensitive to insulin following 16-h exposure (Fig. 2B) but did not cause significant cell loss (not shown).

2.4 Protein synthesis

The rate of *de novo* protein synthesis was determined by tagging newly synthesised proteins with L-azidohomoalanine (Click-iT® AHA, Invitrogen C10102) as published by others [25]. In essence, L6 myoblasts were cultured in 25-cm² flasks to approximately 60% confluency and then exposed to BSA-conjugated palmitate or BSA alone for 16 h. Cells were washed twice with methionine-free DMEM (Invitrogen 21013) supplemented with 2 mM L-glutamine and 1 mM sodium pyruvate, and incubated in this medium for 1 h at 37 °C under carbogen. After this methionine depletion, 25 µM AHA was added and cells were incubated for another 4 h. Cells were harvested by trypsinisation in 1 mL phosphate-buffered saline (PBS) containing 3% (w/v) BSA. After passing cells in this 'flow medium' through a 35-µm cell strainer (Fisher Scientific 08-771-23) they were harvested by centrifugation in 500 µL PBS containing 0.05% (v/v) Triton X-100. After 2-min incubation, permeabilised cells were washed once with flow medium and resuspended in 500 µL Click-iT® cell reaction buffer that was supplemented with CuSO₄ and proprietary additives according to the manufacturer's instructions (Invitrogen C10269) and with 3 µM Alexa Fluor® 488 alkyne (Invitrogen A10267). Cells were incubated for 30 min at room temperature to allow chemoselective ligation between the green-fluorescent alkyne probe and the azido-modified protein. After this, cells were washed once with flow medium and analysed by flow cytometry using a BD FACSAria™ II cell sorter.

2.5 Cellular bioenergetics

2.5.1 Oxygen consumption

Mitochondrial respiratory activity was measured in attached cells as described before [26]. Briefly, L6 myoblasts seeded at 4×10^4 cells per well and exposed to palmitate on XF24 tissue culture plates (Seahorse Bioscience) were washed 4x with a Krebs Ringer Phosphate Hepes buffer (KRPB) comprising 136 mM NaCl, 3.7 mM KCl, 10 mM Hepes, (pH 7.4), 2 mM NaH_2PO_4 , 1 mM MgCl_2 , 1.5 mM CaCl_2 , and 0.1% (w/v) BSA, and were then incubated in this buffer for 1 h at 37°C under air. Human myoblasts were treated similarly, but were seeded at $2\text{--}3 \times 10^4$ cells per well, and were not washed into KRPB, but into serum-free DMEM containing 2 mM glucose and 10 mM Hepes. Subsequently, the plates were transferred to a Seahorse XF24 extracellular flux analyser (controlled at 37°C) for a 10-min calibration after which cellular oxygen consumption was recorded under various conditions to determine both ATP supply and ATP demand (Fig. 1).

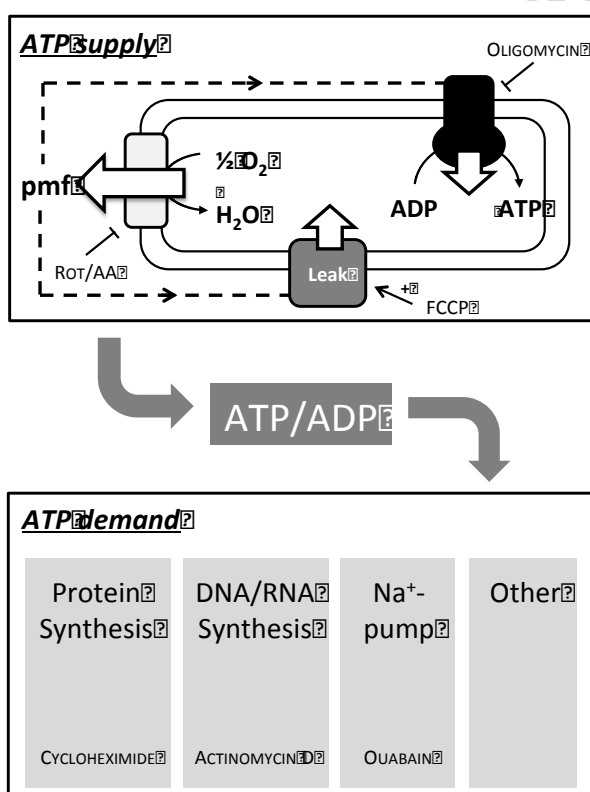


Fig. 1 – Skeletal muscle bioenergetics.

The ATP/ADP ratio in skeletal muscle cells is controlled by ATP demand: changes in ATP-consuming processes are countered by proportional changes in ATP supply. Under aerobic conditions, ATP is mainly supplied by oxidative phosphorylation. Mitochondrial substrate oxidation (measured as rotenone- and antimycin-A-(Rot/AA)-sensitive oxygen uptake) builds a protonmotive force (pmf) across the mitochondrial inner membrane that is either used to make ATP (oligomycin-sensitive oxygen uptake) or is dissipated by proton leak (oligomycin-insensitive oxygen uptake). FCCP renders membranes proton-permeable. Protein synthesis, DNA/RNA synthesis and Na^+ pump activity are ATP-demanding processes that account for about two-thirds of total ATP turnover in L6 and human myoblasts (Figs 6C and 6D). These processes are inhibited by cycloheximide, actinomycin D and ouabain, respectively.

2.5.2 ATP supply

Following Seahorse measurement of basal cellular respiration [26], oligomycin ($5 \mu\text{g}/\text{mL}$), FCCP (trifluorocarbonylcyanide phenylhydrazine – $2 \mu\text{M}$ and $20 \mu\text{M}$ for human and L6 cells, respectively), and a mixture of rotenone ($1 \mu\text{M}$) and antimycin A ($2 \mu\text{M}$) were added sequentially to inhibit the ATP synthase, uncouple oxidative phosphorylation, and to determine non-mitochondrial respiration, respectively (Fig. 1). Non-mitochondrial respiratory

activity was subtracted from all other activities to calculate bioenergetic parameters concerning mitochondrial ATP supply. Cellular respiratory control was calculated as the ratio of FCCP-stimulated and oligomycin-inhibited respiratory rates [27], and coupling efficiency of oxidative phosphorylation was defined as the oligomycin-sensitive part of mitochondrial respiration, i.e., the respiratory proportion that is used to make ATP [27]. Respiration was normalised to cell density derived from DAPI fluorescence [28] to calculate absolute oxygen uptake. Absolute oligomycin-sensitive oxygen consumption rates were converted to ATP supply rates assuming P/O ratios of 2.41 and 2.10 for glucose and palmitate oxidation, respectively [29].

2.5.3 ATP demand

In systems where the ATP/ADP ratio is fully controlled by ATP demand, the activity of an ATP-demanding process may be approximated from the change in oligomycin-sensitive mitochondrial respiratory activity that is seen upon specific inhibition of that process [30,31]. Cycloheximide (40 μ M), actinomycin D (10 μ M) and ouabain (380 μ M) were applied to estimate how much ATP supply flux was allocated to fuel, respectively, protein synthesis, DNA and RNA synthesis, and sodium pump (Na^+/K^+ -ATPase) activity (Fig. 1). The stated inhibitor levels were selected empirically as the lowest concentrations that exerted saturating inhibitory effects on basal mitochondrial respiration without significantly affecting the FCCP-uncoupled respiration.

2.6 Statistics

Mean differences were tested for statistical significance by ANOVA, applying Fisher's LSD multiple comparison post-hoc analysis, using SPSS v17 (IBM) and Stat Graphics Plus v5.1 (Statistical Graphics Corporation) software.

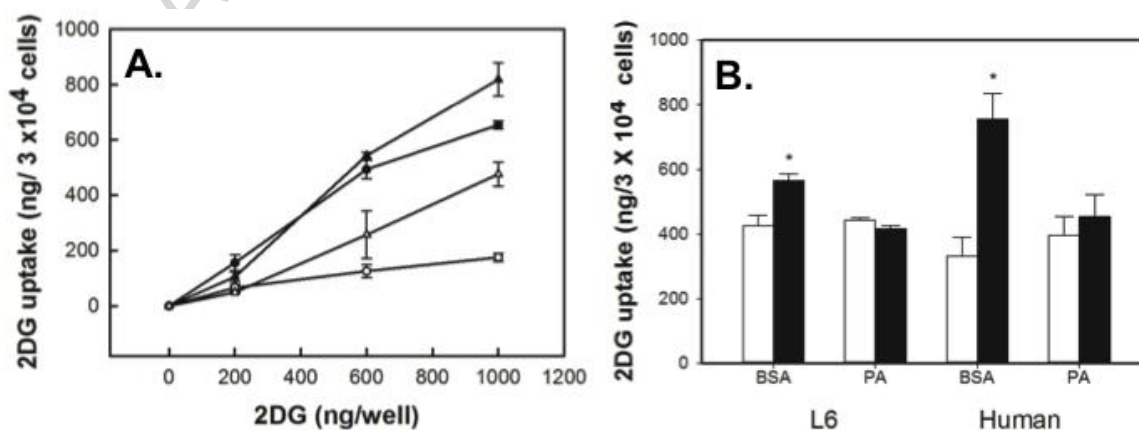


Fig. 2 – Palmitate-induced insulin resistance. *Panel A:* 2DG uptake was measured in L6 (circles) and human (triangles) myoblasts in the absence (white symbols) or the presence of 100 nM insulin (black symbols) as described before [22]. The differences between insulin-exposed and control cells are statistically significant ($P < 0.05$) at applied 2DG levels of 600 and 1000 ng/well. *Panel B:* 2DG

uptake was measured at 30 mg/well in the absence and presence of 100 nM insulin (white and black bars, respectively) in myoblasts exposed to palmitate (PA) or BSA as described in section 2.2. *Differs significantly ($P < 0.05$) from the equivalent condition minus insulin. Data are means \pm SEM of 3 independent experiments.

3. RESULTS

3.1 Palmitate lowers protein synthesis rate

To examine NEFA effects on the energy metabolism of skeletal muscle cells, myoblasts were exposed to palmitate at a dose and exposure time (Material and Methods) that caused insulin resistance (Fig. 2). Control myoblasts respond acutely to insulin as reflected by the stimulatory effect of insulin on dose-dependent 2DG accumulation by L6 and human cells (Fig. 2A). This responsiveness is unaffected when cells are exposed to BSA, but is fully annulled upon exposure to BSA-conjugated palmitate (Fig. 2B).

To explore if the insulin-numbing palmitate exposure is in any way associated with changes in skeletal muscle energy demand, we measured the rate at which L6 cells make protein, a process that represents a significant source of ATP consumption in muscle and other cells [30,32]. Figs 3A and 3B show typical flow cytometry experiments quantifying fluorescence exhibited by control and palmitate-exposed cells, respectively, following 4-h incubation with AHA and subsequent treatment with ALEXA Fluor® 488 alkyne. Control myoblasts clearly contain newly synthesised (AHA-labelled) protein as is reflected by 2 distinct cell populations with median fluorescence values of approximately 8,000 and 20,000 RFU (relative fluorescence units), respectively (Fig. 3A). Fluorescence of cells not exposed to AHA was below 200 RFU (not shown). Palmitate increases the median frequency of the 'low-fluorescence' population from about 250 to 300 counts and decreases the median 'high-fluorescence' frequency from 120 to 60 counts (Fig. 3B). Consequently, the average fluorescence intensity of palmitate-exposed cells is lower than that of control cells (Fig. 3C – 12,500 versus 18,500 RFU), which demonstrates that palmitate has lowered the rate of *de novo* protein synthesis by more than 30%.

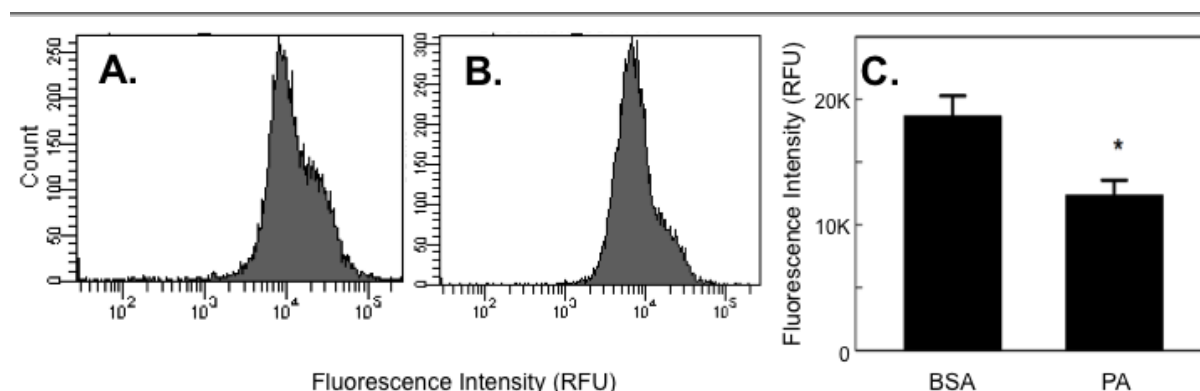


Fig. 3 – Palmitate lowers *de novo* protein synthesis. Control (*Panel A*) and palmitate-exposed (*Panel B*) L6 myoblasts incubated with AHA for 4 h and then treated with ALEXA Fluor® 488 alkyne

were analysed by flow cytometry (10,000 counts per run) applying a excitation/ emission wavelength filter of 495/519 nm. *Panel C*: average fluorescence intensity of cells exposed to BSA or palmitate (PA). Data are means \pm SEM of 4 exposures. *Differs significantly ($P < 0.05$) from the BSA control.

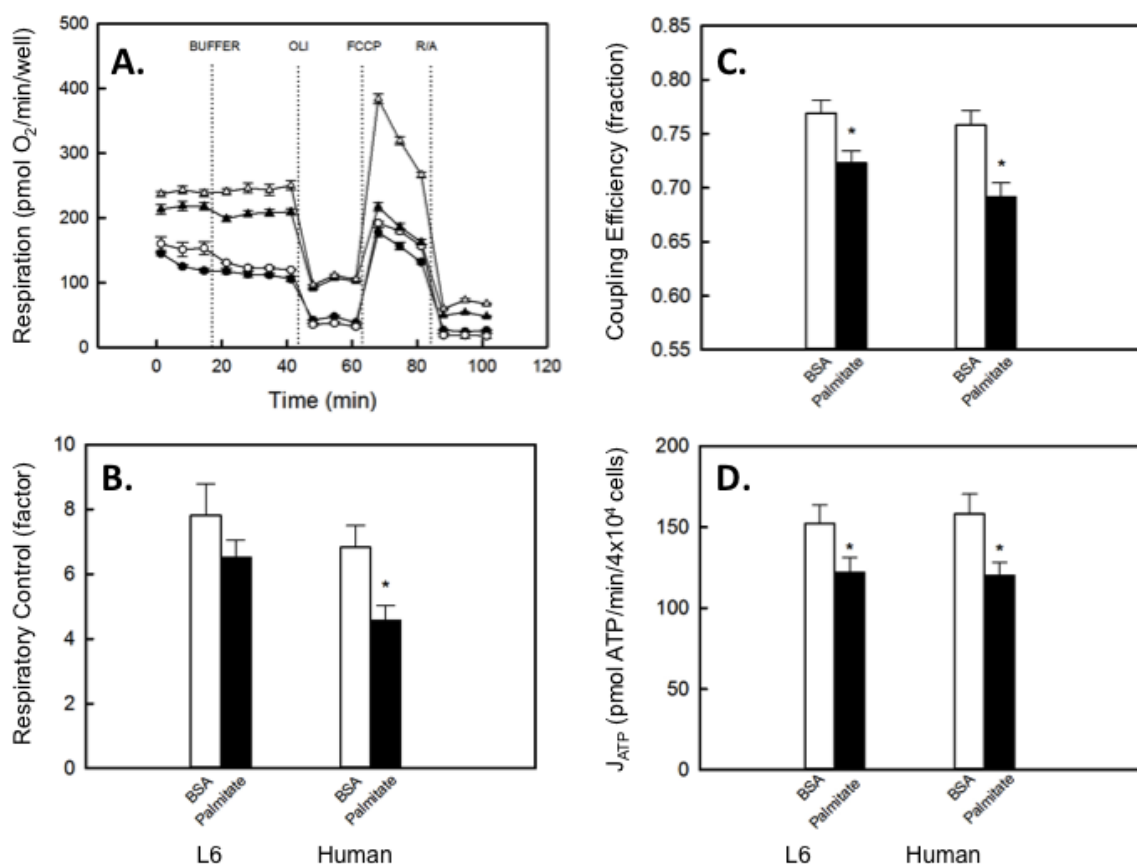


Fig. 4 – Palmitate lowers the rate and efficiency of myoblast ATP synthesis. *Panel A*: typical respiratory traces showing oxygen uptake by L6 (circles) and human (triangles) myoblasts exposed to palmitate (black symbols) or BSA (white symbols). These traces were used as controls in preliminary ATP-demand assays (Fig. 5), which is why buffer was added before oligomycin (OLI), FCCP and rotenone/antimycin A (R/A). Traces were obtained from 1 Seahorse run and are means \pm SEM of 3-4 wells per condition. Cell respiratory control (*Panel B*), coupling efficiency of oxidative phosphorylation (*Panel C*) and the absolute rate of ATP supply (*Panel D*) were derived as described in the text. Data are means \pm SEM of 10 experiments. *Differs significantly ($P < 0.05$) from the equivalent BSA control.

3.2 Palmitate lowers the rate and efficiency of ATP supply

Inhibition of protein synthesis by palmitate (Fig. 3) is expected to change mitochondrial ATP supply, because protein synthesis is a major energy-demanding process in muscle cells [32] and because muscle energy metabolism is predominantly controlled by ATP demand [21]. Respiratory analysis reveals that palmitate-induced insulin resistance indeed coincides with statistically significant changes in oxidative phosphorylation (Fig. 4). Basal cellular oxygen consumption in control cells is inhibited considerably by oligomycin, subsequently stimulated by FCCP, and then almost abolished by antimycin A and rotenone (Fig. 4A). At first glance, these typical respiratory responses are not drastically different in palmitate-exposed cells, although FCCP stimulation of respiration appears attenuated in human myoblasts (Fig. 4A).

Indeed, the apparent palmitate effect on FCCP-uncoupled respiration is reflected by a decreased cell respiratory control ratio [27] in human myoblasts (Fig. 4B). Palmitate exposure also lowers respiratory control in L6 cells, but not to a statistically significant extent (Fig. 4B). In addition, palmitate lowers coupling efficiency of oxidative phosphorylation in human and L6 myoblasts (Fig. 4C), i.e., it decreases the fraction of respiration that is used to make ATP. Absolute ATP synthesis flux is readily derived from oligomycin-sensitive oxygen uptake by normalising it to cell number and multiplying it by P/O. Assuming control cells are fuelled by endogenous glucose (i.e., the sole carbon source fuelling the cells during growth) we used a P/O ratio of 2.41 [29] and calculated that rat and human myoblasts make about 150 pmol ATP per min per 40,000 cells (Fig. 4D). Skeletal muscle suppresses glucose catabolism when lipid is available [33], so using a P/O ratio of 2.10 [29] we established that palmitate lowers the ATP supply rate in both systems to approximately 120 pmol ATP per min per 40,000 cells (Fig. 4D).

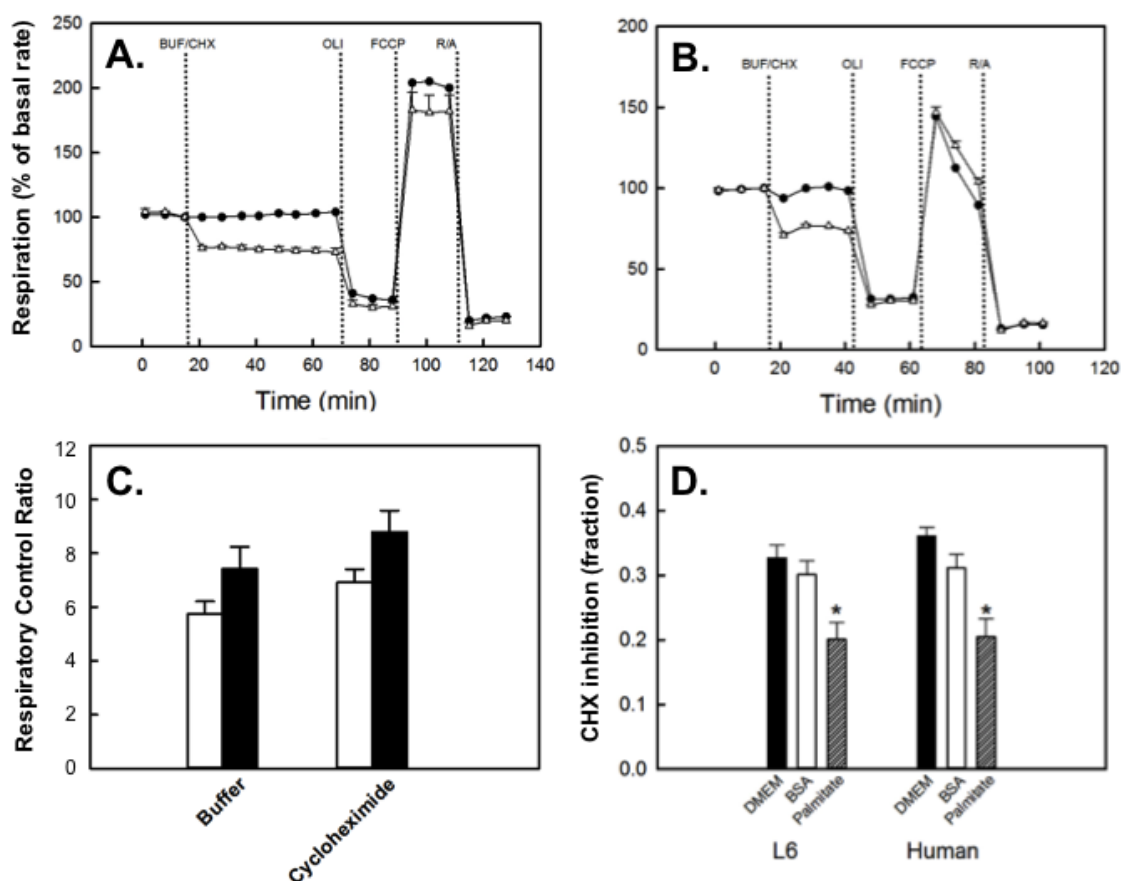


Fig. 5 – Palmitate lowers the proportion of ATP supply allocated to protein synthesis. Typical respiratory traces showing oxygen consumption by L6 (*Panel A*) and human (*Panel B*) myoblasts grown in fully supplemented DMEM (specified in section 2.1). Buffer (BUF – black circles) or 40 μ M cycloheximide (CHX – white triangles) was added before sequential injection of oligomycin (OLI), FCCP and a mix of rotenone and antimycin A (R/A). Traces were obtained from 1 Seahorse run and are means \pm SEM of 3-4 wells per condition. Cell respiratory control ratios (*Panel C* – cf. Material and

Methods) are means \pm SEM of 3 experiments with L6 (white bars) or human (black bars) myoblasts grown in serum-depleted medium containing BSA (*cf.* section 2.2). Sensitivity of basal mitochondrial respiration to cycloheximide (*Panel D* – CHX) was expressed as a fraction of total oligomycin-sensitive respiratory activity. Data are means \pm SEM of 3 experiments with L6 or human myoblasts grown in fully supplemented (*cf.* section 2.1) DMEM (black bars) or in serum-depleted medium with BSA or BSA-conjugated palmitate (white and shaded bars, respectively). *Differs significantly ($P < 0.05$) from the equivalent BSA control.

3.3 Palmitate lowers ATP supply reserved for protein synthesis

A decreased rate of oxidative phosphorylation (Fig. 4) is consistent with palmitate inhibition of protein synthesis (Fig. 3) as lowering ATP supply would be a plausible myoblast response to attenuated energy demand. Indeed, inhibiting ATP turnover will *acutely* lower oligomycin-sensitive respiratory activity of any cell that controls its energy metabolism predominantly by ATP demand [30,31]. Figs 5A and 5B for example demonstrate that 40 μ M cycloheximide causes an instant and stable decrease of basal respiration in both L6 and human myoblasts. Oligomycin lowers respiration further and allows the cycloheximide-induced decrease to be normalised to ATP-synthesis-coupled oxygen uptake (Fig. 5D – DMEM). FCCP uncouples respiration from ATP synthesis and confirms that the respiratory decrease is secondary to lowered ATP demand and not to *direct* inhibition of mitochondrial electron transfer. At a concentration that does not affect the cell respiratory control ratio (Fig. 5C), cycloheximide lowers oligomycin-sensitive respiration by about 35% (Fig. 5D), which indicates that L6 and human cells use one-third of their total ATP supply to drive protein synthesis. BSA tends to lower cycloheximide sensitivity marginally, but palmitate decreases it significantly to $\sim 20\%$ of total respiration linked to ATP synthesis (Fig. 5D). Consistent with measurement of newly made protein (Fig. 3C), palmitate lowers ATP supply reserved for protein synthesis (Fig. 5D).

In a separate set of experiments we also exposed L6 myoblasts to stearate, a saturated fatty acid 2 carbon atoms longer than palmitate, and to oleate and linoleate, the monounsaturated and polyunsaturated counterparts of stearate, respectively. Probably owing to different cell passage number and subtle differences in experimental conditions, coupling efficiency (Fig. 6A) and absolute rate of oxidative phosphorylation (Fig. 6B) in BSA-exposed myoblasts were a little higher than those observed before (Figs 4C and 4D+7D, respectively). Reassuringly, however, these independent results confirm that palmitate significantly lowers the efficiency (Fig. 6A) and the rate (Fig. 6B) of mitochondrial ATP synthesis. Stearate has the same effect on these parameters as palmitate (Figs 6A and 6B). Oleate and linoleate, on the other hand, only tend to lower the ATP synthesis rate (Fig. 6B) and have not effect on coupling efficiency (Fig. 6A). Stearate and linoleate significantly lower cycloheximide sensitivity of mitochondrial respiration linked to ATP synthesis, but less so than palmitate (Fig. 6C). The small negative effect of oleate on cycloheximide sensitivity is not statistically significant. All NEFAs lower the absolute ATP supply flux reserved for protein synthesis (calculated by multiplying the

cycloheximide-sensitive respiration by P/O – see section 3.2), although the effects of oleate and linoleate do not reach statistical significance.

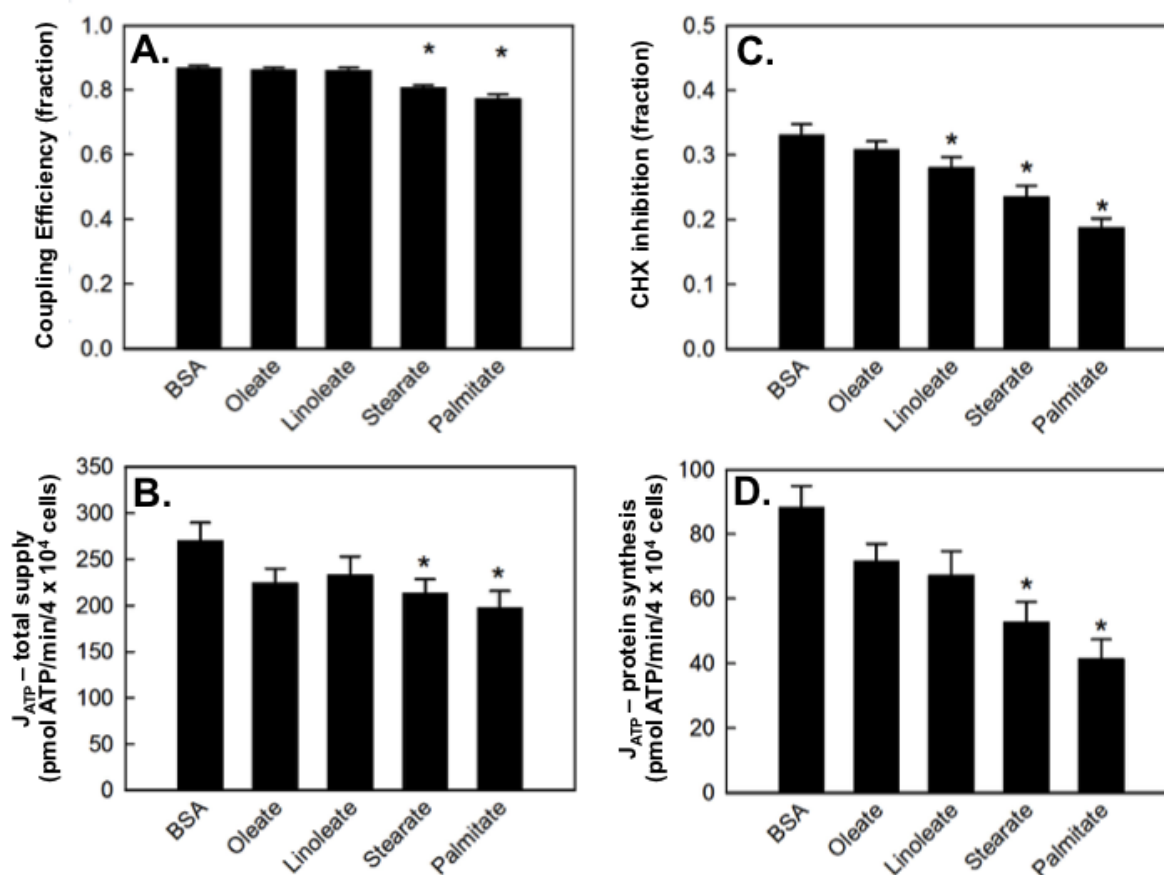


Fig. 6 – Effects of saturated and unsaturated NEFAs on ATP synthesis and ATP turnover in L6 myoblasts. Coupling efficiency of oxidative phosphorylation (*Panel A*), the rate of total mitochondrial ATP synthesis (*Panel B*), cycloheximide (CHX) sensitivity of respiration coupled to ATP synthesis (*Panel C*) and the absolute ATP supply rate used to fuel protein synthesis (*Panel D*) were derived as described in the text. Data are means ± SEM of 4 experiments. *Differs significantly (P < 0.05) from the equivalent BSA control.

3.4 Palmitate causes reallocation of ATP supply

The close agreement between direct (Fig. 3) and indirect (Fig. 5) measurement of palmitate inhibition of myoblast protein synthesis strongly supports the notion that ATP turnover rates can be derived accurately from mitochondrial respiratory analysis [30,31]. Therefore, we also measured ATP supply used for DNA/RNA synthesis and sodium pump activity by quantifying drops in oxygen uptake seen after inhibition of these ATP-consuming processes with 10 μM actinomycin D and 380 μM ouabain, respectively. Similar to cycloheximide, actinomycin D and ouabain inhibit oligomycin-sensitive oxygen uptake without significant effect on FCCP-uncoupled respiration (not shown). Normalising inhibitor-sensitive respiration to cell number and multiplying it by P/O (*cf.* section 3.2) yields the absolute ATP supply flux allocated to the

respective processes (Fig. 7). On average, rat myoblasts use 47, 31 and 26 pmol ATP per min per 40,000 cells to, respectively, fuel protein synthesis, sodium pump activity and DNA/RNA synthesis (Fig. 7A). ATP supply reserved by human cells for protein and DNA/RNA synthesis is similar to that allocated by their rat counterparts, but human myoblasts use comparably little ATP (18 pmol per min per 40,000 cells) to drive the sodium pump (Fig. 7B). Given a total ATP supply of 150 pmol ATP per min per 40,000 cells in this set of experiments (Fig. 4D), it transpires that ~ 70% and 60% of this supply is used by rat and human cells, respectively, to fuel the sum of protein synthesis, DNA/RNA synthesis and sodium pump activity (Figs 7C and 7D); the remaining 30-40% drives processes we have not assessed and thus remains unaccounted.

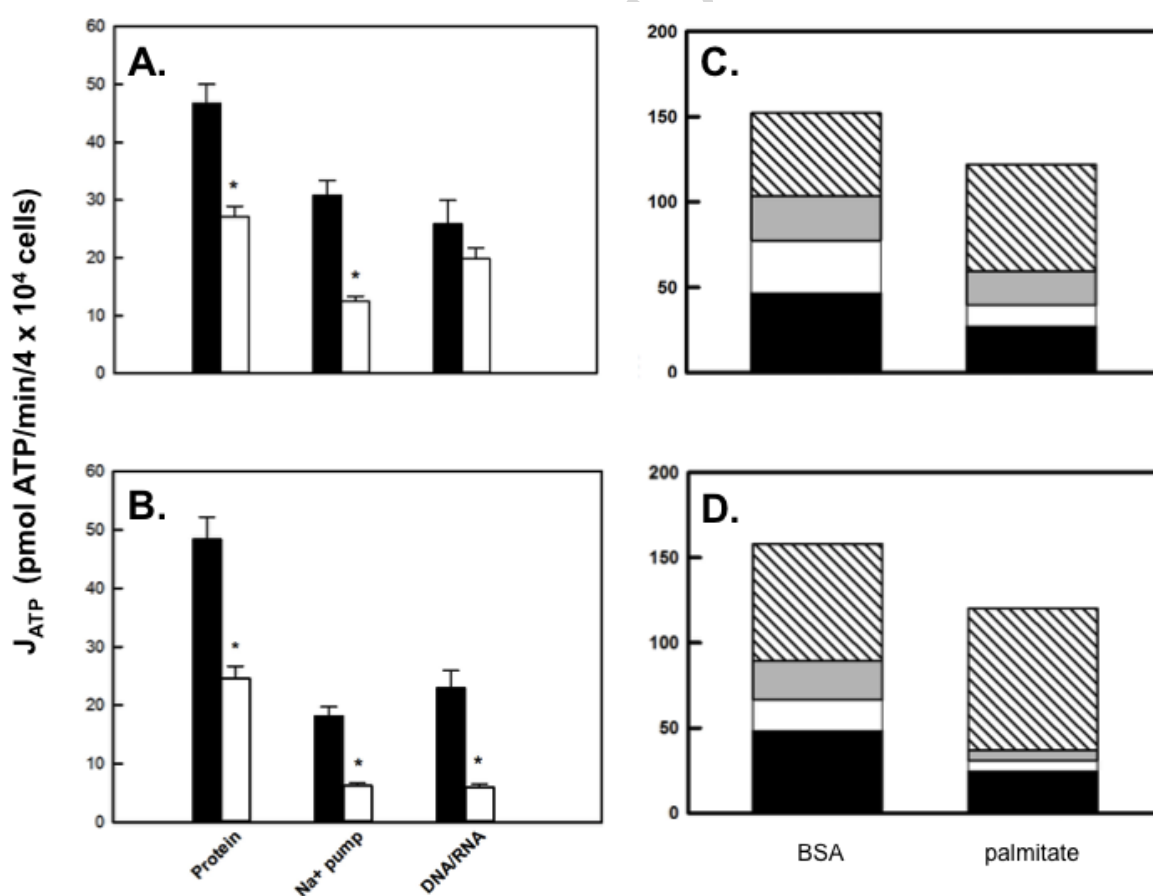


Fig. 7 – Palmitate reallocates ATP supply. Absolute ATP supply rates (J_{ATP}) were calculated as described in the main text in L6 (*Panels A and C*) and human (*Panels B and D*) myoblasts exposed to palmitate (white bars) or BSA (black bars). Oligomycin-sensitive respiration inhibited by cycloheximide, ouabain or actinomycin D was used to calculate ATP supply reserved for protein synthesis, sodium pump activity and DNA/RNA synthesis, respectively. Data are means \pm SEM of 4-6 experiments. *Differs significantly ($P < 0.05$) from the equivalent BSA control. *Panels C and D*: average ATP supply fluxes for protein synthesis (black boxes), sodium pump activity (white boxes), DNA/RNA synthesis (grey boxes) are the same as those shown in *Panels A and B*, respectively. The sum of these fluxes was subtracted from total ATP supply (Fig. 4D) to derive unaccounted ATP demand (shaded boxes).

Palmitate significantly lowers ATP supply for protein synthesis, to about 28 and 24 pmol per min per 40,000 cells in rat and human muscle myoblasts, respectively (Fig. 7). The palmitate effect on absolute ATP supply is a little more pronounced (40-50% inhibition) than its effect on the cycloheximide sensitivity of mitochondrial respiration (Fig. 5D – 33% inhibition), which is owing to the different P/O ratios we used for palmitate-exposed and control cells (section 3.1). Palmitate lowers ATP supply for sodium pump activity by 60-70% and for human (but not rat) DNA/RNA synthesis by almost three-quarters (Fig. 7B). Since the palmitate effect on total ATP supply is lower than its cumulative effect on ATP turnover, palmitate increases the percentage of unaccounted ATP supply in rat (Fig. 7C) and human (Fig. 7D) myoblasts.

4. DISCUSSION

The results reported in this paper reveal that palmitate alters mitochondrial ATP supply and ATP expenditure in rat and human myoblasts (Fig. 8). The data demonstrate that palmitate lowers both the rate and efficiency of ATP supply in these cells (Figs 4 and 6) and, importantly, changes how this supply is allocated between ATP-consuming processes (Fig. 7). Our finding that palmitate and other NEFAs (Fig. 6) remodel ATP turnover is relevant for the causality debate as to mitochondrial involvement in obesity-related insulin resistance.

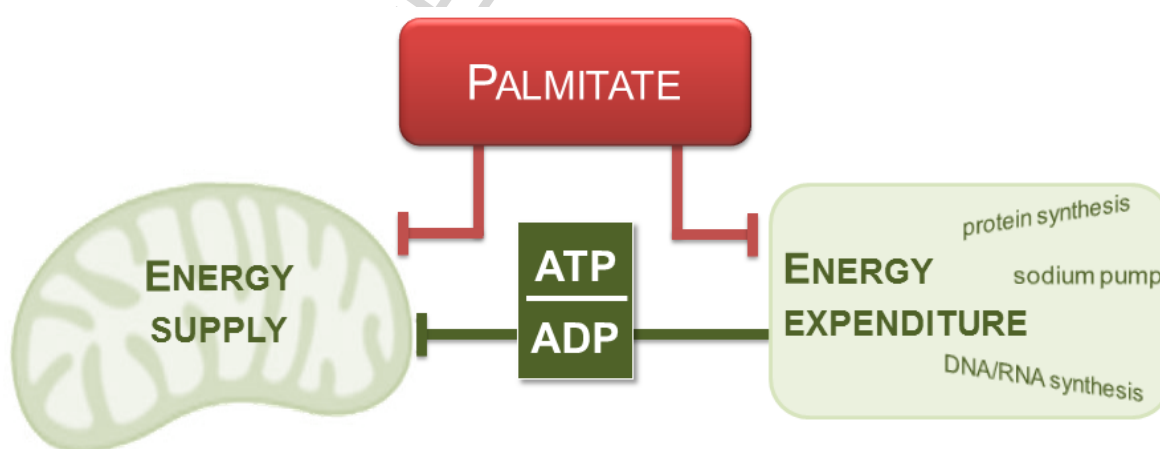


Fig. 8 – Palmitate remodels skeletal muscle bioenergetics. Mitochondrial ATP supply defects emerge directly from harmful palmitate effects on fuel combustion or indirectly from effects on ATP turnover.

4.1 Measurement of ATP demand

ATP turnover measurement from decreases in oligomycin-sensitive respiration provoked by inhibition of ATP-consuming processes ([30,31], Fig. 5) requires careful experimental design. Comparison between direct and indirect protein synthesis measurement for example reveals that ATP supply allocated to this process may readily be overestimated when derived from cycloheximide-sensitive respiration [34]. Overestimation depends on cycloheximide level [34] and thus likely emerges from nonspecific inhibition of fuel oxidation. Such off-site catabolic

effects of ATP demand inhibitors are expected to decrease respiration even when oxygen uptake is uncoupled from ATP synthesis with FCCP, so they would lower cell respiratory control ratios. At the concentrations we applied, cycloheximide, actinomycin D and ouabain did not lower cellular respiratory control, suggesting that inhibition of oligomycin-sensitive oxygen uptake by these compounds was only achieved *indirectly* via their effect on ATP turnover. Initial experiments indicated that these compounds indeed inhibit FCCP-uncoupled respiration when applied at higher levels (not shown). Direct amino acid incorporation measurements show that 25 μM cycloheximide suffices to inhibit protein synthesis [34]. The 40 μM used here is of the same order of magnitude and provokes an instant and relatively stable inhibition (Figs 5A and 5B) that suggests a lack of secondary effects within the timescale of our assay. Importantly, cycloheximide sensitivity of coupled mitochondrial respiration is decreased by one-third when L6 myoblasts are exposed to palmitate (Fig. 5D), i.e., by a magnitude that is identical to the palmitate effect on the protein synthesis rate of these cells (Fig. 3C). This close quantitative agreement between direct and indirect determination of the palmitate effect on protein synthesis strengthens our confidence in the validity of indirect ATP demand measurement.

4.2 Mechanistic considerations

Palmitate lowers coupling efficiency of oxidative phosphorylation (Figs 4C and 6A) and provokes reallocation of ATP supply (Fig. 7) by mechanisms that are presently unclear. The coupling efficiency phenotype likely results from palmitate effects on the proton conductance of phospholipid bilayers [35,36]. Palmitate is for example known to induce transient pores in the mitochondrial inner membrane [37,38] that will increase proton leak and thus lower the proportion of respiration linked to ATP synthesis. The palmitate effect on coupling efficiency is arguably small, but it is worth notice in this respect that our experiments were performed without serum and insulin. We have recently shown that insulin acutely improves mitochondrial function of L6 and human myoblasts by boosting their coupling efficiency of oxidative phosphorylation [22]. Such improvement is annulled in palmitate-exposed cells [22] – the deleterious effect of palmitate on coupling efficiency will therefore be likely amplified in the presence of insulin.

In human and L6 myoblasts, palmitate lowers ATP supply for protein synthesis and sodium pump activity and, in human cells, it also lowers the supply for DNA/RNA synthesis (Fig. 7). Broadly speaking, palmitate could affect ATP turnover in two ways. Skeletal muscle has remarkable remodelling ability that allows functional adaptation to environmental stimuli via activation of diverse signalling pathways [39]. Paths linking nutrient abundance to cell growth are influenced by lipids [40] and it is therefore possible that palmitate down-regulates various ATP-consuming processes *directly*. Alternatively, palmitate may provoke new ATP demand,

which reprioritizes the distribution of myoblast ATP supply. The second explanation predicts that palmitate affects the reported ATP-consuming processes *indirectly*, and is consistent with the increased proportion of unaccounted ATP supply flux seen after palmitate exposure (Figs 6C and 6D). Current efforts are focussed on distinguishing between direct and indirect palmitate effects on ATP expenditure, and on identifying the additional palmitate-induced ATP demand. Activities that possibly account for uninhibited ATP demand are diverse and may include proteolysis, actin/tubulin dynamics and Ca^{2+} -ATPases.

4.3 Mitochondrial insufficiency debate

Despite the incomplete mechanistic understanding of the observed NEFA effects on ATP turnover, our finding that palmitate causes a dramatic reallocation of ATP supply in skeletal muscle (Fig. 7) informs the mitochondrial insufficiency debate. Our data support the slowly emerging awareness [8] that mitochondrial involvement in NEFA-induced insulin resistance cannot be evaluated in a meaningful way if metabolic control is ignored. Mitochondrial capacity *per se* may indeed be sufficient to cope with the lipid load in the obese state [11], but without energy demand this capacity will be inconsequential. This *effective* mitochondrial insufficiency under conditions of low ATP demand will thus allow accumulation of the metabolites that are held responsible for NEFA-induced insulin resistance. We assert that the current 'oxidative capacity', 'redox signalling' and 'mitochondrial load' models of skeletal muscle insulin resistance [8,17] are conceptually the same: lipid metabolites such as diacylglycerol and ceramide [13,14], and ROS [15,16] all, but exclusively, accumulate when mitochondrial substrate supply outweighs energetic needs and thus the effective oxidative phosphorylation capacity.

4.4 Concluding remarks

Our findings highlight that mitochondrial involvement in NEFA-induced insulin resistance of skeletal muscle is best considered in context of bioenergetic control. We have revealed new significant inhibitory effects of palmitate on energy expenditure of rat and human myoblasts. We suggest that the palmitate-decreased rate of ATP supply by oxidative phosphorylation is partly owing to inhibited ATP turnover (Fig. 8). In other words, a seemingly compromised oxidative capacity may have simply arisen from attenuated ATP demand. We believe it may be interesting to explore how palmitate affects skeletal muscle ATP expenditure of different patients as a variable NEFA-sensitivity of ATP turnover could be responsible for a differential propensity of these patients to develop muscle insulin resistance.

ACKNOWLEDGEMENTS

This work was supported by the Medical Research Council [New Investigator Research Grant G1100165 to CA] and Plymouth University [salary support for RBN]. Neither MRC nor Plymouth University were involved in the design and execution of this study, the analysis and interpretation of the data, or in the writing of the manuscript. It was the decision of the authors only to submit the manuscript for publication. We thank Prof. Andrew Jones and Mr Lee Wiley (Sport & Health Sciences, College of Life & Environmental Sciences, University of Exeter) for taking the human skeletal muscle biopsies, Prof. Paul Winyard (Exeter University Medical School, UK) for providing licenced facilities to work with human tissue, and Dr Jane Carré (Plymouth University, UK) for help with the human muscle cell isolation.

AUTHOR CONTRIBUTION

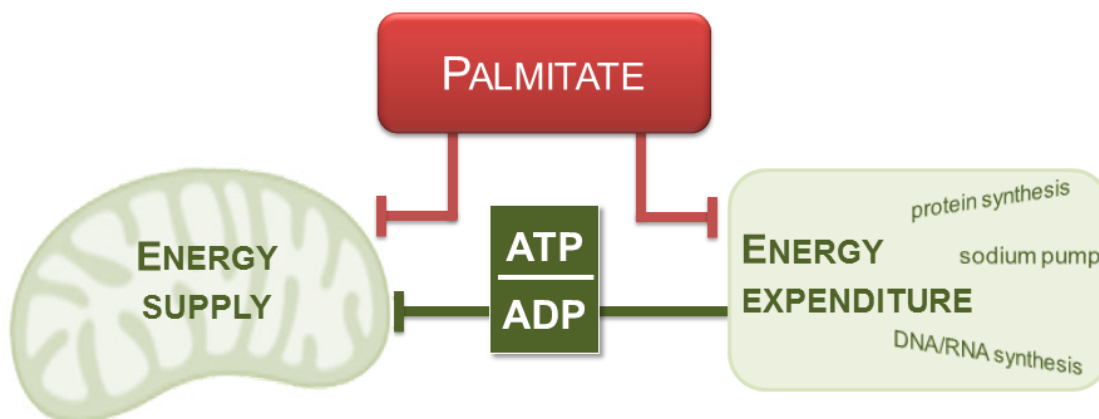
CA conceived and developed the project idea, RBN and CA designed all experiments, RBN executed and analysed all experiments, and produced Figs 2-7, and CA wrote the paper and produced Figs 1 and 8.

REFERENCES

- [1] K.G.M.M. Alberti, P. Zimmet, J. Shaw, IDF Epidemiology Task Force Consensus Group, The metabolic syndrome - a new worldwide definition, *Lancet* 366 (2005) 1059–1062.
- [2] R.H. Unger, Lipotoxicity in the pathogenesis of obesity-dependent NIDDM. Genetic and clinical implications, *Diabetes* 44 (1995) 863–870.
- [3] S.E. Kahn, The relative contributions of insulin resistance and beta-cell dysfunction to the pathophysiology of Type 2 diabetes, *Diabetologia* 46 (2003) 3–19.
- [4] D.M. Muoio, C.B. Newgard, Mechanisms of disease: molecular and metabolic mechanisms of insulin resistance and β -cell failure in type 2 diabetes, *Nat. Rev. Mol. Cell Biol.* 9 (2008) 193–205.
- [5] G. Boden, Obesity and free fatty acids, *Endocrinol. Metab. Clinics North America* 37 (2008) 635–646.
- [6] A.R. Martins, R.T. Nachbar, R. Gorjao, M.A. Vinolo, W.T. Festuccia, R.H. Lambertucci, et al., Mechanisms underlying skeletal muscle insulin resistance induced by fatty acids: importance of the mitochondrial function, *Lipids Health Dis.* 11 (2012) 30.
- [7] J. Szendroedi, E. Phielix, M. Roden, The role of mitochondria in insulin resistance and type 2 diabetes mellitus, *Nat. Rev. Endocrinol.* 8 (2011) 92–103.
- [8] D.M. Muoio, P.D. Neuffer, Lipid-induced mitochondrial stress and insulin action in muscle, *Cell Metab.* 15 (2012) 595–605.
- [9] D.M. Muoio, Metabolic inflexibility: when mitochondrial indecision leads to metabolic gridlock, *Cell* 159 (2014) 1253–1262.
- [10] B.H. Goodpaster, Mitochondrial deficiency is associated with insulin resistance,

- Diabetes 62 (2013) 1032–1035.
- [11] J.O. Holloszy, “Deficiency” of mitochondria in muscle does not cause insulin resistance, *Diabetes* 62 (2013) 1036–1040.
- [12] K. Morino, K.F. Petersen, G.I. Shulman, Molecular mechanisms of insulin resistance in humans and their potential links with mitochondrial dysfunction, *Diabetes* 55 (2006) S9–S15.
- [13] P.M. Coen, B.H. Goodpaster, Role of intramyocellular lipids in human health, *Trends Endocrinol. Metab.* 23 (2012) 391–398.
- [14] V.T. Samuel, G.I. Shulman, Mechanisms for insulin resistance: common threads and missing links, *Cell* 148 (2012) 852–871.
- [15] N. Houstis, E.D. Rosen, E.S. Lander, Reactive oxygen species have a causal role in multiple forms of insulin resistance, *Nature* 440 (2006) 944–948.
- [16] E.J. Anderson, M.E. Lustig, K.E. Boyle, T.L. Woodlief, D.A. Kane, C.-T. Lin, et al., Mitochondrial H₂O₂ emission and cellular redox state link excess fat intake to insulin resistance in both rodents and humans, *J. Clin. Invest.* 119 (2009) 573–581.
- [17] K.H. Fisher-Wellman, P.D. Neuffer, Linking mitochondrial bioenergetics to insulin resistance via redox biology, *Trends Endocrinol. Metab.* 23 (2012) 142–153.
- [18] A. Wredenberg, C. Freyer, M.E. Sandström, A. Katz, R. Wibom, H. Westerblad, et al., Respiratory chain dysfunction in skeletal muscle does not cause insulin resistance, *Biochem. Biophys. Res. Comm.* 350 (2006) 202–207.
- [19] J.A. Pospisilik, C. Knauf, N. Joza, P. Benit, M. Orthofer, P.D. Cani, et al., Targeted deletion of AIF decreases mitochondrial oxidative phosphorylation and protects from obesity and diabetes, *Cell* 131 (2007) 476–491.
- [20] C. Zechner, L. Lai, J.F. Zechner, T. Geng, Z. Yan, J.W. Rumsey, et al., Total skeletal muscle PGC-1 deficiency uncouples mitochondrial derangements from fiber type determination and insulin sensitivity, *Cell Metab.* 12 (2010) 633–642.
- [21] D.G. Nicholls, S. Ferguson, *Bioenergetics* 4, Academic Press, London, 2013.
- [22] R.B. Nisr, C. Affourtit, Insulin acutely improves mitochondrial function of rat and human skeletal muscle by increasing coupling efficiency of oxidative phosphorylation, *Biochim. Biophys. Acta.* 1837 (2014) 270–276.
- [23] J.K. Ching, P. Rajguru, N. Marupudi, S. Banerjee, J.S. Fisher, A role for AMPK in increased insulin action after serum starvation, *Am. J. Physiol. - Cell Physiol.* 299 (2010) C1171–C1179.
- [24] A.H. Huber, J.P. Kampf, T. Kwan, B. Zhu, A.M. Kleinfeld, Fatty acid-specific fluorescent probes and their use in resolving mixtures of unbound free fatty acids in equilibrium with albumin, *Biochemistry* 45 (2006) 14263–14274.
- [25] D.C. Dieterich, A.J. Link, J. Graumann, D.A. Tirrell, E.M. Schuman, Selective identification of newly synthesized proteins in mammalian cells using bioorthogonal noncanonical amino acid tagging (BONCAT), *Proc. Nat. Acad. Sci.* 103 (2006) 9482–9487.
- [26] C. Affourtit, M.D. Brand, Measuring mitochondrial bioenergetics in INS-1E insulinoma cells, *Meth. Enzymol.* 457 (2009) 405–424.

- [27] M.D. Brand, D.G. Nicholls, Assessing mitochondrial dysfunction in cells, *Biochem. J.* 435 (2011) 297–312.
- [28] J. Barlow, V. Hirschberg Jensen, C. Affourtit, Uncoupling protein-2 attenuates palmitoleate protection against the cytotoxic production of mitochondrial reactive oxygen species in INS-1E insulinoma cells. *Redox Biol.* 4 (2015) 14–22.
- [29] M.D. Brand, The efficiency and plasticity of mitochondrial energy transduction, *Biochem. Soc. Trans.* 33 (2005) 897–904.
- [30] F. Buttgereit, M.D. Brand, A hierarchy of ATP-consuming processes in mammalian cells, *Biochem. J.* 312 (1995) 163–167.
- [31] M.J. Birket, A.L. Orr, A.A. Gerencser, D.T. Madden, C. Vitelli, A. Swistowski, et al., A reduction in ATP demand and mitochondrial activity with neural differentiation of human embryonic stem cells, *J. Cell Sci.* 124 (2011) 348–358.
- [32] P.G. Arthur, J.J. Giles, C.M. Wakeford, Protein synthesis during oxygen conformance and severe hypoxia in the mouse muscle cell line C2C12, *Biochim. Biophys. Acta.* 1475 (2000) 83–89.
- [33] P.J. Randle, Regulatory interactions between lipids and carbohydrates: the glucose fatty acid cycle after 35 years, *Diab. Metab. Rev.* 14 (1998) 263–283.
- [34] W. Wieser, G. Krumschnabel, Hierarchies of ATP-consuming processes: direct compared with indirect measurements, and comparative aspects, *Biochem. J.* 355 (2001) 389–395.
- [35] V.P. Skulachev, Uncoupling: new approaches to an old problem of bioenergetics, *Biochim. Biophys. Acta.* 1363 (1998) 100–124.
- [36] V.N. Samartsev, Fatty acids as uncouplers of oxidative phosphorylation, *Biochemistry Mosc.* 65 (2000) 991–1005.
- [37] G.D. Mironova, E. Gritsenko, O. Gateau-Roesch, C. Levrat, A. Agafonov, K. Belosludtsev, et al., Formation of palmitic acid/ Ca^{2+} complexes in the mitochondrial membrane: a possible role in the cyclosporin-insensitive permeability transition, *J. Bioenerg. Biomembr.* 36 (2004) 171–178.
- [38] G.D. Mironova, N-E.L. Saris, N.V. Belosludtseva, A.V. Agafonov, A.B. Elantsev, K.N. Belosludtsev, Involvement of palmitate/ Ca^{2+} (Sr^{2+})-induced pore in the cycling of ions across the mitochondrial membrane, *Biochim. Biophys. Acta.* 1848 (2015) 488–495.
- [39] R. Bassel-Duby, E.N. Olson, Signaling pathways in skeletal muscle remodeling, *Annu. Rev. Biochem.* 75 (2006) 19–37.
- [40] R. Zoncu, A. Efeyan, D.M. Sabatini, mTOR: from growth signal integration to cancer, diabetes and ageing, *Nat. Rev. Mol. Cell Biol.* 12 (2010) 21–35.



Graphical abstract

ACCEPTED

Highlights

- Lipotoxic palmitate exposure lowers rate and efficiency of myoblast ATP synthesis.
- Palmitate decreases the activity of major ATP-consuming processes in myoblasts.
- Palmitate causes reallocation of ATP supply in human and rat myoblasts.

ACCEPTED MANUSCRIPT